

DOI: 10.1070/QEL16045

Third harmonic generation in the short-wavelength UV range by a single plasmonic nanostructure

P.N. Melentiev, A.A. Kuzin, A.E. Afanasiev, V.I. Balykin

Abstract. **The nonlinear optical interaction of laser radiation with nanostructures formed in gold and aluminium nanofilms has been experimentally studied. It is shown that, despite the high susceptibility χ_3 of aluminium in comparison with gold, the third-harmonic generation efficiency at a wavelength of 260 nm is much higher for the nanostructures formed in a gold nanofilm because of the efficient excitation of a localised plasmon resonance at the fundamental frequency.**

Keywords: *harmonic generation, UV spectral range, plasmon resonance, nanofilm.*

1. Introduction

Plasmonic metal nanostructures are basic elements of nanoplasmonics. The small geometric sizes of nanostructures limit the motion of free electrons of the metal, which leads to the formation of spatial electron oscillation modes (localised plasmon resonances) with resonant frequencies lying in a wide spectral range: from the UV region to microwaves.

Localised plasmon resonances are determined by the motion of a very large number of electrons involved in collective oscillations of the nanostructure electron cloud (the resonance oscillator strength $f \sim 10^5$). The interaction of a nanostructure with laser radiation at the frequencies of its localised plasmon resonance leads to large electric field amplitudes near the nanostructure, which exceed the field amplitude in the incident wave. Thus, the nanostructure makes it possible to localise energy in regions much smaller in size than the light wavelength [1, 2]. There are various practical applications of this local field amplification: optical microscopy with a nanoscale resolution [3, 4], biosensors [5], optical nanolithography [6], photovoltaics [7], and light registration and photodetectors [8].

P.N. Melentiev, V.I. Balykin Institute of Spectroscopy, Russian Academy of Sciences, ul. Fizicheskaya 5, Troitsk, 142190 Moscow, Russia; Institute on Laser and Information Technologies, Russian Academy of Sciences, ul. Pionerskaya 2, Troitsk, 142190 Moscow, Russia; e-mail: balykin@isan.troitsk.ru;
A.A. Kuzin Institute of Spectroscopy, Russian Academy of Sciences, ul. Fizicheskaya 5, Troitsk, 142190 Moscow, Russia; Moscow Institute of Physics and Technology (State University), Institutskii per. 9, 141700 Dolgoprudnyi, Moscow region, Russia;
A.E. Afanasiev Institute of Spectroscopy, Russian Academy of Sciences, ul. Fizicheskaya 5, 142190 Troitsk, Moscow, Russia

Received 8 February 2016
Kvantovaya Elektronika **46** (5) 414–418 (2016)
Translated by Yu.P. Sin'kov

When considering the dynamics of electrons in a solid, it is important to separate collective electron oscillations from the dynamics of screened electrons. For example, the Hamiltonian characterising the interaction between electrons in a solid can be written as a sum of two terms [9]:

$$H = \sum_{ij(i\neq j)} \frac{e^2}{|\boldsymbol{r}_i - \boldsymbol{r}_j|} = \sum_{ij(i\neq j)} \left\{ \sum_{|\boldsymbol{r}_i - \boldsymbol{r}_j| > \lambda_{\min}}{}' + \sum_{|\boldsymbol{r}_i - \boldsymbol{r}_j| < \lambda_{\min}} \right\} \frac{e^2}{|\boldsymbol{r}_i - \boldsymbol{r}_j|}, \quad (1)$$

where the $\lambda_{\min}$ value is determined by the charge screening in the electron plasma. It is impossible to excite plasmonic waves with a wavelength smaller than the charge screening length (Debye length) $l_D = v_F/\omega_p$ in a solid, where v_F is the electron velocity on the Fermi surface, and ω_p is the plasma frequency [9]. The summation over the electrons (plasmons) involved in collective oscillations and the summation over the pairs of electrons located within the charge screening sphere are explicitly separated in expression (1). The total Hamiltonian of electron interaction includes also (along with the aforementioned summands) a term describing the interaction of screened electrons with collective electron oscillations [9].

An example of practical application of the dynamics of individual (screened) electrons in plasmonic nanostructures is single-photon [10–12] and multiphoton [13–16] luminescence. The photoluminescence in metals is the result of interaction of light with metal, which is determined by the corresponding interband and intraband transitions and the dynamics of individual (screened) electrons [10–12]. Currently, the interest in the photoluminescence is caused by the possibility of using metal nanoparticles as theragnostic biomarkers, because they simultaneously make it possible to perform microscopy of deep tissues and can be used for local heating in the phototherapy of cells [17–19]. However, screened electrons in nanoplasmonics applications, interacting with collective electron oscillations (plasmons), are responsible for one of the channels of plasmon energy (Landau) loss [20].

In strong laser fields, the motion of free electrons of plasmonic nanostructures is characterised by large oscillation amplitudes. As a result, anharmonicity manifests itself in the motion of the electron cloud, and, as a consequence, an effective nonlinear dipole moment arises in the nanostructure [21]. Well-known results of nonlinear optical interaction of laser radiation with nanostructures are harmonic generation [22–29] and parametric frequency mixing [30–33].

It was demonstrated in [34] that, controlling the nanostructure geometry, one can control the character of its nonlinear optical interaction with laser radiation. For example, the formation of a nanostructure with roughness having a characteristic size of about 10 nm may leads to dominance of the individual-electron dynamics; as a consequence, nonlin-

ear optical interaction manifests itself as multiphoton luminescence. The radiation from the nanostructure has a large spectral width. When a nanostructure has a smooth surface, the interaction scenario is radically different. In this case, the interaction of a nanostructure with a laser beam is generally characterised by coherent dynamics of free electrons (plasmons). The result of this interaction is the generation of spectrally narrow harmonics.

The main problem related to the practical application of optical nonlinearity of plasmonic nanostructures is its low efficiency (large optical losses in metal lead to fast heating of nanostructure and, as consequence, cause its catastrophic melting [35]). In practice, the laser beam intensity at the fundamental frequency is limited by a value of $\sim 10^{10}$ W cm^{-2}. The record values of harmonic generation efficiency are on the order of $\sim 10^{-6}$ [29, 34, 36], which, at first glance, seems to be very low. However, one must also take into account the extremely small nanostructure volume with which laser radiation interacts. With allowance for this circumstance, the harmonic generation efficiency in a nanostructure, reduced to its volume, is unprecedentedly high; it exceeds by more than six orders of magnitude the corresponding value for the nonlinear materials widely used in optics, such as $LiIO_3$, KDP, KTP, or $LiNbO_3$ [37].

The UV-harmonic generation by nanoparticles is of particular practical importance. First, based on this process, one can design nanolocalised UV radiation sources, which are necessary for nanodiagnostics and nanolithography. Second, the high optical nonlinearity of nanoparticles in the UV range can be used in cell phototherapy [38].

2. Generation of UV light by plasmonic nanostructures

The generation of UV light by plasmonic nanostructures has been studied poorly. There are only few experimental studies in this field [39–41], where third harmonic generation in nanostructures excited by a Ti:sapphire laser was reported. In particular, a UV photon flux of 10^4 photons s^{-1} from a single gold nanostructure was obtained in [41].

Gold is the most widespread plasmonic material. However, recent studies showed that the optical nonlinearity of aluminium greatly exceeds that of gold. In particular, it was shown in [42, 43] that aluminium susceptibility χ_3 at a wavelength of 1550 nm is three orders of magnitude higher than the corresponding value for gold, while at a wavelength of 780 nm the difference is two orders of magnitude [44]. Thus, one would expect aluminium nanostructures to be more efficient (in comparison with gold nanoparticles) THG sources in the UV range. In this paper, we report the results of studying the THG by gold and aluminium nanostructures.

Significant drawbacks of metal nanostructures as nonlinear elements of localised radiation sources are as follows: (i) the presence of a strong background of excitation radiation at the fundamental frequency and (ii) the destruction of nanostructures at high powers of incident radiation, which, in turn, limits significantly the efficiency of the nonlinear process. An example of a nanoobject that is free of these drawbacks and, at the same time, exhibits high nonlinear properties, is a nanohole in a metal film.

According to the Babinet principle, the optical properties of a nanohole in an ideal metal can be directly related to the properties of a metal nanodisk that is complementary to the nanohole (i.e., has the same sizes) [45]. However, a nanohole in a metal screen has a number of advantages for applications in nonlinear nanoplasmonics [34, 42]. These are, first, a weak background from the excitation radiation, which is significantly attenuated because of the low nanohole transmittance, and, second, the resistance to high-power radiation due to the efficient heat sink in the metal film where the nanohole is formed [42].

The purpose of this study was to design a nanolocalised THG source in the UV region. To this end, we investigated nanostructures in the form of a nanoslit formed in a gold or aluminium film. In accordance with the Babinet principle, these nanoslits are complementary to nanorods, which are most widespread in nanoplasmonics. As well as a nanorod, a nanoslit may possess two plasmon resonances, which are excited by light beams polarised along the nanoslit and perpendicular to it [1].

Figure 1 shows the results of calculating the electric field amplification in nanoslits exposed to a plane monochromatic wave with a wavelength of 780 nm. The calculations were performed by the finite-difference time-domain (FDTD) method. The nanoslit parameters (see Fig. 1) were chosen based on the experimental results, because a maximum THG signal was obtained specifically for the nanoslits with the reported geometric sizes. One can see that the field gain in the nanoslit formed in a gold film is $E/E_0 = 4$, whereas for the nanoslit formed in an aluminium film the gain is $E/E_0 = 1.09$. This difference is due to the fact that gold has better plasmonic properties at a wavelength of 780 nm in comparison with aluminium.

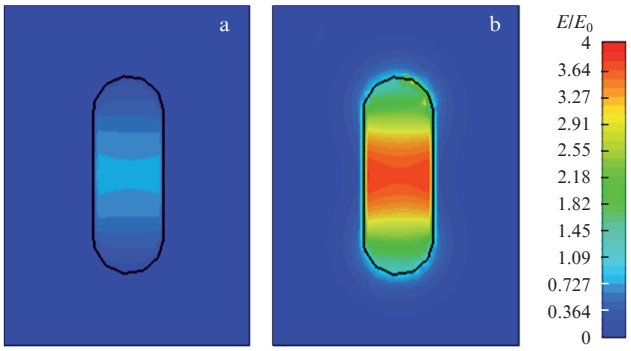

Figure 1. Results of calculating the electric field gain in nanoslits exposed to a plane monochromatic wave with a wavelength of 780 nm: (a) a nanoslit 80×225 nm in size, formed in a 200-nm-thick Al film, and (b) a nanoslit 80×175 nm size, formed in a 200-nm-thick Au film.

3. Experimental results and discussion

Nanostructures in the form of nanoslits were fabricated in aluminium and gold nanofilms (both 200 nm thick) using a focused ion beam. Nanofilms were grown by thermal deposition in a vacuum chamber at a pressure of 10^{-6} Torr. The nanoslits in both films had the same geometry; their width was 80 nm, and the length was varied from 75 to 525 nm with a step of 25 nm. Scanning electron microscopy (SEM) images of the experimental samples with nanoslits are presented in Figs. 2b–2d. To verify the reproducibility of the experimental results, 16 nanoslits of each size were formed in each nanofilm. The distance between nanoslits was chosen to be 10 μm. This distance exceeds several times the spot diameter for a

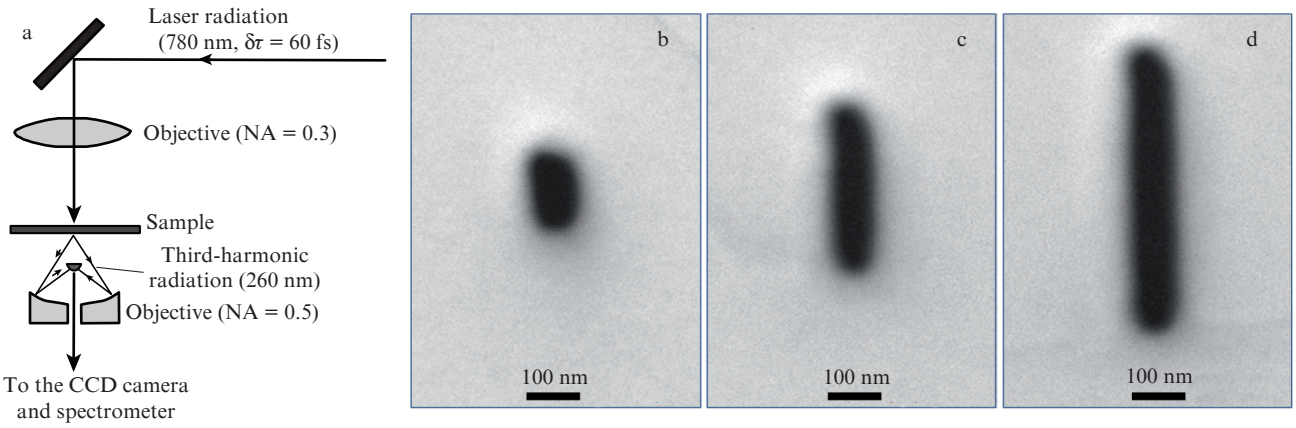

Figure 2. (a) Schematic of the experiment and (b–d) SEM images of nanoslits of identical width and lengths of (b) 150, (c) 325 and (d) 550 nm, formed in a gold film.

strongly focused excitation laser beam. This geometry allowed us to investigate experimentally the THG from individual nanostructures.

A schematic of the experimental setup for studying the THG from nanoslits in the laser beam field is shown in Fig. 2a. A 60-fs laser pulse with a centre wavelength of 780 nm was focused by an objective ($15^{\times}$, NA = 0.3) into a spot 2.5 μm in diameter on the surface of a sample, located in the object plane of an inverted microscope. The maximum value of laser peak intensity at which the samples remained undamaged was 10^{11} W cm^{-2}.

The optical inverted microscope for simultaneous studies in the visible and UV spectral ranges was developed based on a Nikon Eclipse commercial microscope. UV quartz lenses, aluminium mirrors, and mirror objectives were installed in the microscope. The radiation emitted by the nanostructure was collected by a mirror objective ($40^{\times}$, NA = 0.5) and analysed using a CCD camera or a spectrometer equipped with a Hamamatsu CCD camera, the quantum efficiency of which exceeded 20% in the UV range. To suppress the fundamental frequency signal, a bandpass filter with a centre wavelength of 260 nm and a transmission band of 60 nm was installed after the objective. This microscope makes it possible to perform optical measurements in the spectral range from 220 to 950 nm.

Figure 3a shows the transmission spectrum of an individual nanohole 150 nm in diameter, formed in a 200-nm-thick gold film deposited on the surface of ultrathin (40 nm) silicon oxide membrane [46, 47]. The use of an ultrathin membrane is necessary to form a through nanohole (both in the nanofilm and in the membrane) transmitting 260-nm light. The measured spectrum contains three emission lines of a mercury lamp, which indicates that the microscope designed can be used for UV measurements.

We investigated the THG in samples of three types: a bare substrate (without a deposited metal film), a substrate coated by a metal (gold or aluminium) film without nanostructures, and a substrate coated by a metal film with nanostructures. The THG signal was detected from only the samples with nanostructures. Thus, the THG efficiency of nanostructures exceeds greatly the THG efficiency of the dielectric substrate and metal nanofilm.

A characteristic THG spectrum of a nanoslit is shown in Fig. 3b. It can be seen that the measured spectrum contains a peak at a wavelength of 260 nm, which amounts to

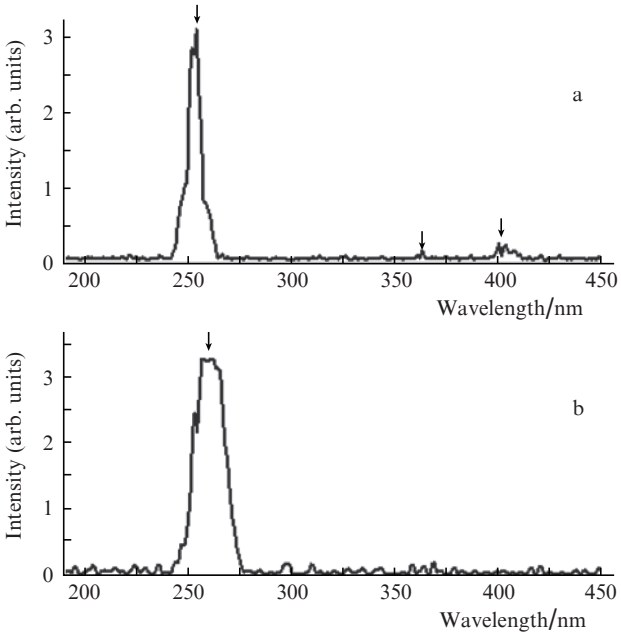

Figure 3. Spectra of (a) mercury lamp radiation transmitted through a nanohole 150 nm in diameter and (b) THG from an individual nanoslit. The arrows indicate the mercury lamp lines.

1/3 of the fundamental radiation wavelength. The measured dependence of the THG signal from nanoslits on the pump intensity is approximated well by a cubic dependence, which confirms the three-photon character of the signal recorded. Thus, the spectrum in Fig. 3b is indeed a THG spectrum.

Figure 4 shows the measured values of THG efficiency for nanoslits of different lengths, fabricated in gold and aluminium nanofilms. It can be seen that the THG efficiency depends strongly on the nanoslit length. The highest efficiency is detected for a 175-nm nanoslit formed in the gold nanofilm and for a 225-nm nanoslit formed in the aluminium nanofilm. As follows from our calculations, a plasmon resonance is excited at the fundamental frequency in nanoslits of specifically these sizes. The plasmon resonance excitation leads to a large increase in the field amplitude at the fundamental frequency and, as a consequence, to a higher THG efficiency.

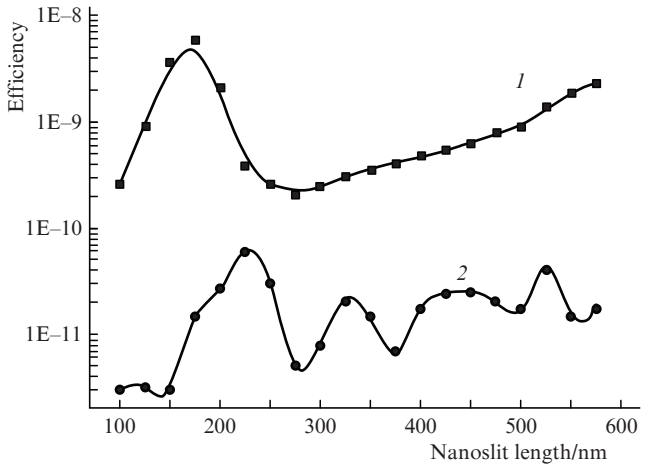

Figure 4. THG efficiencies of nanoslits of different lengths, formed in (*1*) Au and (*2*) Al nanofilms.

Our measurements showed that the third-harmonic photon flux from a 175-nm-long nanoslit formed in a gold nanofilm is $P = 9\times10^5$ photons s^{-1}. This value is two orders of magnitude larger than the known THG data on gold nanorods [41]. Specifically the use of the complementary geometry of nanostructure (nanoslit) allowed us to increase significantly the field intensity at the fundamental frequency and, consequently, increase greatly the radiation power at the third-harmonic frequency.

As follows from Fig. 4, the THG efficiency of the nanoslits formed in a gold nanofilm exceeds by two orders of magnitude the corresponding efficiency of the nanoslits in the aluminium nanofilm. This fact is surprising, because the coefficient χ_3 for aluminium at the fundamental frequency (780 nm) is known to be two orders of magnitude larger than the corresponding value for a gold film [42, 43]. Therefore, the THG efficiency of the nanostructures formed in an aluminium nanofilm was expected to exceed greatly that of the nanostructures formed in a gold nanofilm. Specifically the efficient excitation of plasmon resonance at the fundamental frequency in gold and, in contrast, a small increase in the field amplitude at the fundamental frequency in aluminium (which has an absorption peak at a wavelength of 780 nm) explain the significant advantage of gold as an efficient THG source in the UV spectral range.

4. Conclusions

The nonlinear optical interaction of Ti : sapphire laser radiation with individual nanostructures formed in aluminium and gold nanofilms was investigated. The chosen nanostructure geometry makes it possible to implement a plasmon resonance at the laser frequency, which leads to THG radiation in the UV spectral range at a wavelength of 260 nm. It was found that, as a result of the efficient excitation of plasmon resonance in gold nanostructures and the loss in aluminium at the Ti : sapphire laser wavelength, the THG efficiency of gold nanostructures is two orders of magnitude higher than that of the nanostructures formed in an aluminium nanofilm. It was shown that a nanoslit in a gold nanofilm may serve as a nanolocalised radiation source in the UV spectral region with an unprecedentedly high photon flux: $P = 9\times10^5$ photons s^{-1}.

Acknowledgements. The work was supported in part by the 'Extreme Light Fields' Programme of the Presidium of the Russian Academy of Sciences, the Programme of the Government of the Russian Federation for Support of Research under the Guidance of Leading Scientists (Grant No. 14.B25.31.0019), and the Russian Science Foundation (Grant No. 14-12-00729).

References

1. Novotny L., van Hulst N. *Nat. Photonics*, **5**, 83 (2011).
2. Giannini V., Fernàndez Domìnguez A.I., Heck S.C., Maier S.A. *Chem. Rev*., **111**, 3888 (2011).
3. Gerton J.M., Wade L.A., Lessard G.A., Ma Z., Quake S.R. *Phys. Rev. Lett*., **93**, 180801 (2004).
4. Frey H.G., Witt S., Felderer K., Guckenberger R. *Phys. Rev. Lett.*, **93**, 200801 (2004).
5. Anker J.N., Hall W.P., Lyandres O., Shah N.C., Zhao J., Van Duyne R.P. *Nat. Mater*., **7**, 442 (2008).
6. Fedoruk M., Meixner M., Carretero-Palacios S., Lohmüller T., Feldmann J. *ACS Nano*, **7**, 7648 (2013).
7. Atwater H.A., Polman A. *Nat. Mater.*, **9**, 205 (2010).
8. Tang L., Kocabas S.E., Latif S., Okyay A.K., Ly-Gagnon D.-S., Saraswat K.C., Miller D.A.B. *Nat. Photonics*, **2**, 226 (2008).
9. Levich V.G., Vdovin Yu.A., Myamlin V.A. *Kurs teoreticheskoi fiziki* (Course of Theoretical Physics) (Moscow: Nauka, 1971) Vol. 2, p. 834.
10. Mooradian A. *Phys. Rev. Lett.*, **22**, 185 (1969).
11. Dulkeith E., Niedereichholz T., Klar T.A., Feldmann J., von Plessen G., Gittins D.I., Mayya K.S., Caruso F. *Phys. Rev. B*, **70**, 205424 (2004).
12. Melentiev P.N., Konstantinova T.V., Afanasiev A.E., Kuzin A.A., Baturin A.S., Balykin V.I. *Opt. Express*, **20**, 19474 (2012).
13. Ghenuche P., Cherukulappurath S., Taminiau T.H., van Hulst N.F., Quidant R. *Phys. Rev. Lett*., **101**, 116805 (2008).
14. Bouhelier A., Beversluis M.R., Novotny L. *Appl. Phys. Lett.*, **83**, 5041 (2003).
15. Schuck P., Fromm D.P., Sundaramurthy A., Kino G.S., Moerner W.E. *Phys. Rev. Lett*., **94**, 017402 (2005).
16. Melentiev P., Afanasiev A., Kuzin A., Zablotskiy A., Balykin V. *Opt. Express*, **23**, 11444 (2015).
17. Nagesha D., Laevsky G., Lampton P., Banyal R., Warner C., DiMarzio C., Sridhar S. *Int. J. Nanomed.*, **2**, 813 (2007).
18. Durr N., Larson T., Smith D., Korgel B., Sokolov K., Ben-Yakar A. *Nano Lett.*, **7**, 941 (2007).
19. Gobin A., Lee M., Halas N., James W., Drezek R., West J. *Nano Lett.*, **7**, 1929 (2007).
20. Khurgin J.B. *Faraday Discuss*., **178**, 109 (2015).
21. Fomichev S., Popruzhenko S., Zaretsky D., Becker W. *Opt. Express*, **11**, 2433 (2003).
22. Capretti A., Pecora E.F., Forestiere C., Negro L.D., Miano D. *Phys. Rev. B*, **89**, 125414 (2014).
23. Czaplicki R., Mäkitalo J., Siikanen R., Husu H., Lehtolahti J., Kuittinen M., Kauranen M. *Nano Lett*., **15**, 530 (2015).
24. Bouhelier A., Beversluis M., Hartschuh A., Novotny L. *Phys. Rev. Lett*., **90**, 013903 (2003).
25. Lippitz M., van Dijk M.A., Orrit M. *Nano Lett*., **5**, 799 (2005).
26. Kim S., Jin J., Kim Y.J., Park I.-Y., Kim Y., Kim S.W. *Nature*, **453**, 757 (2008).
27. Bar-Elli O., Grinvald E., Meir N., Neeman L., Oron D. *ACS Nano*, **9**, 8064 (2015).
28. Aouani H., Rahmani M., Navarro-Cía M., Maier S. *Nat. Nanotech*., **9**, 290 (2014).
29. Aouani H., Navarro-Cía M., Rahmani M., Maier S.A. *Adv. Opt. Mater*., **3**, 1059 (2015).
30. Palomba S., Novotny L. *Nano Lett*., **9**, 3801 (2009).
31. Danckwerts M., Novotny L. *Phys. Rev. Lett*., **98**, 026104 (2007).
32. DOI:10.1364/OME.5.002217.
33. Melentiev P.N., Afanasiev A.E., Kuzin A.A., Gusev V.M., Kompanets O.N., Esenaliev R.O., Balykin V.I. *Nano Lett*., **16**, 1138 (2016).
34. Melentiev P.N., Afanasiev A.E., Kuzin A.A., Baturin A.S., Balykin V.I. *Opt. Express*, **21**, 13896 (2013).

35. Link S., Wang Z., El-Sayed M. *J. Phys. Chem. B*, **104**, 7867 (2000).
36. Metzger B. et al. *Nano Lett*., **14**, 2867 (2014).
37. DOI: 10.1038/ncomms1805.
38. Sasanpour P., Rashidian B., Rashidian B., Vossoughi M. *Nano*, **5**, 325 (2010).
39. Xu T., Jiao X., Blair S. *Opt. Express*, **17**, 23582 (2009).
40. N'Gom M., Ye J.Y., Norris T.B., Agarwal A., Kotov N. *Proc. Conf. Quantum Electron. Laser Science, 2009* (Baltimore, MD, 2009).
41. Schwartz O., Oron D. *Nano Lett*., **9**, 4093 (2009).
42. Melentiev P., Konstantinova T., Afanasiev A., Kuzin A., Baturin A., Tausenev A., Konyaschenko A., Balykin V. *Laser Phys. Lett*., **10**, 075901 (2013).
43. Konstantinova T.V., Melentiev P.N., Afanas'ev A.E., Kuzin A.A., Starikov P.A., Baturin A.S., Tausenev A.V., Konyashchenko A.V., Balykin V.I. *Zh. Exp. Teor. Fiz*., **117**, 21 (2013).
44. Castro-Lopez M., Brinks D., Sapienza R., Van Hults N.F. *Nano Lett*., **11**, 4674 (2011).
45. Born M., Wolf E. *Principles of Optics: Electromagnetic Theory of Propagation, Interference and Diffraction of Light* (Cambridge: University Press, 1999).
46. Melentiev P.N., Zablotskiy A.V., Lapshin D.A., Sheshin E.P., Baturin A.S., Balykin V.I. *Nanotechnol.*, **20**, 235301 (2009).
47. Melentiev P.N., Zablotskiy A.V., Kuzin A., Lapshin D.A., Baturin A.S., Balykin V.I. *Metamaterials*, **3**, 157 (2009).